Comprehensive analysis of R-spondin fusions and *RNF43* mutations implicate novel therapeutic options in colorectal cancer.

Running title: Molecular analysis of RSPO/RNF43 positive colorectal cancer.

Andreas Seeber[1,*,+], Francesca Battaglin[2,+], Kai Zimmer[1,+], Florian Kocher[1+], Yasmine Baca[3], Joanne Xiu[3], Gilbert Spizzo[1,4], Veronica Novotny-Diermayr[5], Dietmar Rieder[6], Alberto Puccini[7], Jeff Swensen[3], Michelle Ellis[3], Richard M. Goldberg[8], Axel Grothey[9], Anthony F. Shields[10], John L. Marshall[11], Benjamin A. Weinberg[11], Paul E. Sackstein[11], Kiat Hon Lim[12], Gek San Tan[12], Chadi Nabhan[3], W. Michael Korn[3], Arno Amann[1], Zlatko Trajanoski[6], Martin D. Berger[13], Emil Lou[14], Dominik Wolf[1], and Heinz-Josef Lenz[2]

[1] Department of Hematology and Oncology, Comprehensive Cancer Center Innsbruck, Medical University of Innsbruck, Innsbruck, Austria
[2] Norris Comprehensive Cancer Center, Keck School of Medicine, University of Southern California, Los Angeles, CA, USA
[3] Caris Life Sciences, Phoenix, AZ, USA
[4] Department of Internal Medicine, Oncologic Day Hospital, Hospital of Bressanone-Brixen, Bressanone-Brixen, Italy
[5] Experimental Drug Development Centre (EDDC), A*Star, Singapore
[6] Biocenter, Institute of Bioinformatics, Medical University of Innsbruck, Innsbruck, Austria
[7] Oncologia Medica 1, Ospedale Policlinico San Martino – IRCCS, Genova, Italy
[8] West Virginia University Cancer Institute, Morgantown, WV, USA
[9] West Cancer Center, Germantown, TN, USA
[10] Department of Oncology, Karmanos Cancer Institute, Wayne State University, Detroit, MI, USA
[11] Ruesch Center for The Cure of Gastrointestinal Cancers, Lombardi Comprehensive Cancer Center, Georgetown University Medical Center, Washington, DC, USA
[12] Translational Pathology Centre, Department of Molecular Pathology, Singapore General Hospital, Singapore
[13] Department of Medical Oncology, Inselspital, Bern University Hospital, University of Bern, Bern, Switzerland
[14] Divison of Hematology and Oncology, University of Minnesota, MS, USA

+ These authors contributed equally

Funding: This work was supported by the National Cancer Institute (P30CA 014089).
Keywords: Wnt, colorectal cancer, RNF43, RSPO, R-spondin, molecular profile

Conflict of interests: FB, KZ, GS, FK, DR, AP, BAW, PES, KHL, AG, GST, HT, SHL, HLN, AA, ZT, MDB, and DW have no competing interests. AFS has received research funding, travel payments, and is on the speaker's panel for Caris. AS, RMG, JLM, EL, HJL has received travel payments, and is on the speaker`s panel for Caris. YB, JX, JS, ME, CN, and WMK are employers of Caris. VND is employer of A*Star.

***Corresponding author:**
Andreas Seeber, MD, PhD - Department of Hematology and Oncology, Comprehensive Cancer Center Innsbruck - Medical University of Innsbruck - Anichstrasse 35, 6020 Innsbruck, Austria

Email: andreas.seeber@tirol-kliniken.at - Tel: 0043 50504 83166

Translational Relevance:

To provide meaningful rationales to develop new impactful targeted approaches for colorectal cancer (CRC) patients, we comprehensively described the mutational landscape of R-spondin fusion proteins (*RSPOfp*) and *RNF43* mutations, which are known to induce Wnt signaling. Using a cohort of 7,245 CRC samples we could identify five new *RSPO* rearrangements and could describe the unique molecular portrait of *RSPOfp* and *RNF43* mutations in CRCs. The genetic profile of *RSPOfp* positive tumors is similar to *RNF43*-mutated CRC and is characterized by a higher frequency of *BRAF*, *SMAD4* and *KMT2D* mutations in comparison to *RSPOfp/RNF43* negative cases. Of note, a subgroup of *RNF43*-mutated tumors is associated with microsatellite instability. Our data could support clinical and pre-clinical research developing treatments targeting the Wnt pathway and could also provide a rationale for combinational approaches to overcome primary resistance to immunotherapy in CRC.

ABSTRACT:

Purpose: Gene fusions involving R-spondin (*RSPOfp*) and *RNF43* mutations have been shown to drive Wnt-dependent tumor initiation in colorectal cancer (CRC). Herein, we aimed to characterize the molecular features of *RSPOfp/RNF43*mutated (mut) compared to wildtype CRCs to gain insights into potential rationales for therapeutic strategies.

Experimental design: A discovery cohort was classified for *RSPOfp/RNF43* status using DNA/RNA sequencing and immunohistochemistry. An independent cohort was used to validate our findings.

Results: The discovery cohort consisted of 7,245 CRC samples. *RSPOfp* and *RNF43* mutations were detected in 1.3% (n=94) and 6.1% (n=443) of cases. We found 5 *RSPO* fusion events that had not previously been reported (e.g. *IFNGR1-RSPO3*). *RNF43*-mut tumors were associated with right-sided primary tumors. No *RSPOfp* tumors had *RNF43* mutations. In comparison to wildtype CRCs, *RSPOfp* tumors were characterized by a higher frequency of *BRAF*, *BMPR1A* and *SMAD4* mutations. *APC* mutations were observed in only a minority of *RSPOfp*-positive compared to wildtype cases (4.4 vs. 81.4%). Regarding *RNF43* mutations, a higher rate of *KMT2D* and *BRAF* mutations were detectable compared to wildtype samples. While *RNF43* mutations were associated with a microsatellite instability (MSI-H)/mismatch repair deficiency (dMMR) phenotype (64.3%), and a TMB ≥10 mt/Mb (65.8%), *RSPOfp* was not associated with MSI-H/dMMR. The validation cohort replicated our genetic findings.

Conclusions: This is the largest series of *RSPOfp/RNF43*-mut CRCs reported to date. Comprehensive molecular analyses asserted the unique molecular landscape associated with *RSPO/RNF43* and suggested potential alternative strategies to overcome the low clinical impact of Wnt-targeted agents and immunotherapy.

INTRODUCTION:

Colorectal cancer (CRC) remains one of the major causes of cancer specific morbidity and mortality worldwide (1, 2). Despite therapeutic improvements, the prognosis of patients with metastatic disease remains poor with a 5-year overall survival (OS) rate of approximately 14% (1). Thus, new therapeutic strategies are urgently needed to improve survival.

Activation of the Wnt/β-catenin pathway, mostly facilitated by genetic mutations encoding for the adenomatous polyposis coli (APC) protein, can initiate tumorigenesis in CRC (3, 4). *In vitro* experiments have determined that the restoration of functional *APC* leads to tumor regression even in CRC cells with additional oncogenic mutations (i.e. *TP53* or *KRAS*) (5). Therefore, Wnt/β-catenin signaling represents a major oncogenic driver in CRC. Over the last years, different genetic alterations activating the Wnt signaling pathway have been discovered. Seshagiri and colleagues (6) described chromosomal rearrangements involving members of the R-spondin family (*RSPO*) in CRC for the first time, which can be observed in up to 8% of CRCs. Studies suggest that such *RSPO* translocations alone are sufficient to initiate carcinogenesis (7), as are mutations in *RNF43*, a negative feedback regulator of the Wnt/β-catenin pathway. *RSPO* molecules bind to the G-protein coupled receptor (LGR) family (LGR4/5/6) which contains a leucine-rich repeat segment resulting in an up-regulation of the Wnt/β-catenin pathway by sequestering the E3 ubiquitin ligase *RNF43* (8). Mutations in *RNF43* have been described in a variety of malignancies, including CRC and gastric cancer, with a frequency of up to 20% (9-15). Interestingly, the frequency of *RNF43* mutations was noted to be even higher in microsatellite-unstable cancers (11). Most of the loss-of-function (LOF) mutations in *RNF43* have been determined to lead to an increased cell surface abundance of the Wnt receptor Frizzled, rendering the cells dependent upon Wnt/β-catenin

signaling (16). Therefore, these cells are suggested to be more sensitive to inhibition of the porcupine homolog (PORCN) protein (16), a posttranslational modificator of the Wnt protein (17).

RSPOfp-positive*/RNF43*-mutated (mut) tumors represent a distinct genetic subgroup of CRCs. However, gene alterations co-occurring in this subgroup are largely unknown. Thus, we set up this study to define the molecular profile of *RSPO/RNF43*-positive CRC that may provide important insights how Wnt/β-catenin pathway deregulation drives tumor growth in CRC. For this, we performed extensive genomic and transcriptomic sequencing, as well as immunohistochemistry (IHC), to compare molecular profiles of *RSPO/RNF43*-positive vs. wildtype (WT) cases, and detected clusters of gene mutation associations as well as several relations with microsatellite instability (MSI-H) and tumor mutation burden (TMB).

MATERIALS AND METHODS:

Sample characterization of the discovery cohort

Colorectal carcinoma specimens of 7,245 patients were submitted to Caris Life Sciences (Phoenix, AZ, USA) for genomic profiling. These cases were retrospectively reviewed, and gene sequencing, amplification and protein expression data were analyzed. The pathology report was included with the specimens and H&E slides were prepared for each tumor sample to be reviewed by board-certified pathologists to confirm the diagnosis of CRC. Tumors with a histologic diagnosis that was not concordant with the diagnosis of CRC were excluded from this analysis. During the recruitment period, tests have varied since there were different requests by the treating physicians and the testing technologies continuously evolved over time. The next generation sequencing (NGS) platform for tumors tested in 2015 or earlier used the MiSeq platform (45 genes included) while those tested after 2015 were

sequenced with the NextSeq platform (592 genes included). In keeping with 45 CFR 46.101(b) this study was performed utilizing retrospective, de-identified clinical data. Therefore, this study is considered IRB exempt and no patient consent was necessary from the subjects. Thus, only basic demographic information was available. Patients were stratified into *RSPOfp* or *RNF43* positive and negative cases. *RNF43* mutations included only pathogenic or presumed pathogenic mutations. Tumors with benign *RNF43* mutations, presumed benign *RNF43* mutations, or *RNF43* variants of unknown significance were categorized as *RNF43*-WT. Germline testing could not be performed due to the lack of access to germline DNA.

Samples of the validation cohort

A total of 816 cases of CRCs were recruited between January 2016 and December 2017 at the Singapore General Hospital, Singapore. A local Ethics Committee approval was obtained. Molecular profiling was analyzed for *RNF43* mutations (excluding the specific G569fs variant) and co-mutations in Wnt and MEK signaling pathways as well as MSI-H or mismatch repair deficiency (dMMR) (MSI-H/dMMR). *RSPO* fusions were not characterized.

Analyses performed

Immunohistochemistry (IHC) was performed on 1,258 tumor samples on formalin-fixed paraffin-embedded (FFPE) sections on glass slides for the discovery cohort. Four micrometer sections were mounted on slides and stained using an automated system (Benchmark, Ventana Medical Systems, Tucson, AZ; Autostainer, DAKO, Carpinteria, CA) according to manufacturer's instructions, and were optimized and validated per CLIA/CAP and ISO requirements. All proteins of interest were evaluated on tumor cells. An intensity score (0 = no staining; 1+ = weak staining; 2+ = moderate staining; 3+ = strong staining) and a

proportion score to determine the percentage of cells staining positive (0-100%) was used. The primary antibody used to detect PD-L1 expression was SP142 (Spring Biosciences, CA, USA). The staining was deemed positive if its intensity on the membrane of the tumor cells was ≥2+ and the percentage of positively stained cells was ≥5%. Results were classified as positive or negative by using previously defined thresholds specific to each marker, based on published clinical literature that associates biomarker status to specific treatment response. The primary antibody used for PD-L1 testing was MRQ-22 (Ventana) and staining was scored as positive if the number of PD-L1 positive cells was >1 cell per high power field. A single board-certified pathologist independently evaluated immunohistochemical results.

NGS was performed on FFPE tumor samples using the NextSeq platform (Illumina, Inc., San Diego, CA). A custom-designed SureSelect XT assay was used to enrich 592 whole-gene targets (Agilent Technologies, Santa Clara, CA). All variants were detected with >99% confidence based on allele frequency and amplicon coverage with an average sequencing depth of coverage of >500 and with an analytic sensitivity of 5%. Genetic variants identified were interpreted by board-certified molecular geneticists and categorized as 'pathogenic,' 'presumed pathogenic,' 'variant of unknown significance,' 'presumed benign,' or 'benign,' according to the American College of Medical Genetics and Genomics (ACMG) standards. When assessing mutation frequencies of individual genes, 'pathogenic,' and 'presumed pathogenic', were defined as mutations while 'benign' or 'presumed benign' variants and 'variants of unknown significance' were defined as wild type.

A combination of multiple test platforms was used to determine the MSI or MMR status of the tumors profiled, including fragment analysis (FA, Promega, Madison, WI), IHC (MLH1, M1 antibody; MSH2, G2191129 antibody; MSH6, 44 antibody; and PMS2, EPR3947 antibody [Ventana Medical Systems, Inc., Tucson, AZ, USA]) and NGS (for tumors tested with NextSeq

platform, 7,000 target microsatellite loci were examined and compared to the reference genome hg19 from the University of California).

Statistics

Statistical comparisons were performed with the Chi-square test and the Mann-Whitney U test when appropriate. A two-sided p-value < 0.05 was considered as statistically significant. P-values were further corrected for multiple comparison using the Benjamini-Hochberg method to avoid type I error, and an adjusted p-value (q-value) of <0.05 was considered as a significant difference.

Real-world overall survival information was obtained from insurance claims data in an updated larger cohort (incorporating the initially described discovery cohort) and calculated from first specimen collection to last contact. Kaplan-Meier estimates were calculated for the molecularly defined patient cohorts.

Availability of data and materials

The deidentified sequencing data are owned by Caris Life Sciences. The datasets generated during and analyzed during the current study are available from the authors upon reasonable request and with permission of Caris Life Sciences. Qualified researchers may contact the corresponding author with their request.

RESULTS

Patients` characteristics and prognosis

In total, 7,245 CRC patients were tested for alterations in *RSPO* and *RNF43* (see **Table 1**). Of those, 443 (6.1%) and 94 patients (1.3%) showed a *RNF43* mutation or a *RSPOfp*, respectively. *RSPO3* fusions were more frequently detected than *RSPO2* translocations (89 vs. 5 cases).

Patients with a *RSPOfp* were younger than patients harboring a *RNF43* mutation (61 vs. 69 years, p=0.0003). No difference in distribution by gender was noted between *RSPOfp* and wildtype (WT) cases (p=n.s.). For *RNF43* mutations, a significant female predominance was observed compared to male patients (p<0.001). Furthermore, we found a higher percentage of cases with *RNF43* mutations in right-sided than in left-sided CRC (14.3 vs. 3.1%, p<0.001). However, no site-specific difference was observed for *RSPOfp*.

The most frequently detected *RSPOfp* was the *PTPRK-RSPO3* fusion protein (n=89). Of note, we detected 5 fusion partners (*CPSF1*, *CDH17*, *MATN2* and *ADAM9*) which had not been described before (see **Supplementary Table 1**). The most frequently detected point mutations in *RNF43* was G659fs, followed by R117fs and P660fs (see **Supplementary Table 2**).

Until now, the prognostic relevance of *RNF43* mutations and *RSPOfp* remains largely unclear. Therefore, we performed survival analyses using real-world data obtained from insurance claims. CRC patients harboring a *RNF43* mutation or a *RSPOfp* are associated with a poor survival compared to WT cases **(Figure 1AB)**. Moreover, in the MSS sub-cohort patients harboring *RSPOfp* or *RNF43* mutations were characterized by poor survival (*RSPOfp* vs. WT: HR 0.61, 95%CI 0.47-0.79, p<0.001; *RNF43*-mut vs. WT: HR 0.65, 95%CI 0.57-0.75, p<0.001).

Molecular landscape of *RSPO* fusion proteins and *RNF43* mutations

RSPOfp-positive CRCs were associated with a higher rate of co-incident mutations in *BRAF* (35.9 vs. 6.3%), *SMAD4* (30.0 vs. 13.5%), *BMPR1A* (5.4 vs. 0.2%), *AKT1* (3.3 vs. 0.4%) and *ERBB3* (5.4 vs. 1.6%, all q<0.05) compared to WT cases (**Figure 2A**).

Compared to *RNF43*-mut cancers, co-incident mutations in *TP53* (79.1%), *KRAS* (53.3%), and *SMAD4* (30.0%) occurred more frequently in *RSPOfp*-positive cancers (*RNF43*: 54.1%, 18.8%

and 15.3%, respectively; all q<0.05). Importantly, in *RSPOfp*-positive CRCs we discovered no concomitant *RNF43* mutations. In contrast, tumors containing *RNF43* mutations exhibited a different molecular landscape as compared to *RSPOfp*-positive tumors: *ARID1A* (75.6 vs. 35.7%), *ASXL1* (65.8 vs. 6.3%), *BRAF* (53.6 vs. 35.9%), *KMT2D* (43.3 vs. 2.5%), and *PTEN* (18.2 vs. 4.3%) gene alterations were more frequently detected (all q<0.05). Of note, *APC* mutations were observed in 19.3% of *RNF43*-mut cases, in 4.4% of *RSPOfp*-positive tumors and in 81.4% of WT cases (all q<0.05). Regarding *BRAF* mutations the most prevalent genetic variant was the V600E mutation (78.8%).

Copy number alterations (CNAs) in *MYC* and *AKT2* genes were differently distributed between *RSPOfp*-positive tumors compared to *RNF43*-mut tumors (4.4 vs. 1.1%, and 2.2 vs. 0.0%, respectively; all q<0.05). Amongst others, CNAs in *CDX2* gene were found more often in WT cases (11.3%) than in *RSPOfp*-positive (3.3%) or *RNF43*-mut (2.3%) samples (all q<0.05) (**Figure 2B**).

Validation cohort

An independent validation cohort was used to confirm our findings in terms of *RNF43* mutations. The retrospective use of a next generation sequencing panel without analyses on fusions prohibited further validation of the findings generated in the *RSPOfp* subset of the discovery cohort. The validation cohort consisted of 816 CRC patients (**Table 2**). This cohort was obtained from a time period between 2016 and 2017 and was retrospectively analyzed. The data was mined for molecular status of *RNF43* and other mutations including *APC*, *KRAS*, *BRAF*, *NRAS,* and other genes. MSI-H/dMMR was also included in this analysis. In line with the findings from our discovery cohort, the incidence of *RNF43* mutations was similar (7.97% vs. 6.1%, p=n.s.). Moreover, the co-activation of Wnt and MAPK signaling (including, *APC*,

KRAS, *BRAF* and *NRAS*) was strongly associated with *RNF43* mutations (in total: 88%); 12% had no detectable coincident mutations. Of the *RNF43*-mut cases, 11% showed a MSI-H/dMMR status, 64% showed a MSS/pMMR status, while 25% had no data for MSI-H/dMMR status available.

RNF43 mutations are associated with microsatellite instability

Next, we analyzed biomarkers associated with a predictive value for response to immune checkpoint inhibitors. In samples harboring a *RSPO fusions,* no individual with a MSI-H/dMMR genotype was detected (0.0%), compared to a MSI-H/dMMR rate of 64.3% in *RNF43*-mut samples (q<0.001), and 2.3% in WT tumors (q<0.001) (**Figure 2C**). Moreover, in *RSPOfp*-positive tumors no case presented with a tumor mutational burden (TMB) of ≥10 mt/Mb. However, in *RNF43*-mut samples, 65.8% had a TMB ≥10 mt/Mb (q<0.001), which was also higher than for WT cases (4.8%, q<0.001). Positive staining for PD-L1 was detected in 15.7% of *RSPOfp*-positive specimens, 19.1% of *RNF43*-mut samples, and 2.7% of WT cases (q<0.001 for *RSPOfp* vs. WT, and *RNF43*-mut vs. WT).

Since MSI-H/dMMR status may trigger secondary mutations, we performed a subgroup analysis in MSS cases. A higher prevalence of females and right-sided primary locations in the MSS subset of patients harboring a *RNF43* mutation was observed. Comparing the molecular profile of the *RSPOfp*-positive and the MSS/*RNF43*-mut cases, no differences in the frequency of *TP53* mutations (79.1 vs. 85.2%, p=n.s.) and *BRAF* mutations (35.9 vs. 43.7%, p=n.s.) were observed. However, there were more *KRAS* mutations in the *RSPOfp*-positive group than in the MSS/*RNF43*-mut group (53.3 vs. 24.2%, q<0.001). Moreover, the rate of *APC* mutations in the MSS/*RNF43*-mut subgroup was only 11.5%, compared to 81.6% in MSS/WT cases (q<0.01) (**Figure 3A**). Interestingly, in the MSS/*RNF43*-mut subgroup, *ARID1A*

and *ASXL1* mutations were identified in 22.7% and 2.2%, respectively, compared to 75.6% and 65.8% in the overall *RNF43*-mut cohort.

In the MSS/*RNF43*-mut subgroup (n=158) and MSS*/RNF43/RSPOfp* WT cases (n=6,533), only 6.4% of the *RNF43*-mut samples and 2.6% of the WT samples had a TMB ≥10 mt/Mb (q<0.001). Furthermore, PD-L1 positive staining was observed in 12.9% of the MSS/*RNF43*-mut subgroup and in 2.4% of the MSS WT samples (q<0.001) (**Figure 3B**). In terms of CNA within the MSS subgroup, we observed more frequent CDX2 CNAs within the *RNF43/RSPO* WT (11%) compared to *RSPOfp*-positive (3%) and *RNF43*-mut (6%) cancers (all, q<0.05). In contrast, CNAs in *TFEB*, *AKT2*, *HNRNPA2B1* as well as in *HSP90AB1* were frequently less detected in *RNF43/RSPO* WT compared to *RNF43/RSPO*-positive tumors (all, q<0.05) (**Figure 3C**).

Regarding the MSI-H/dMMR subcohort it revealed that patients harbouring *RNF43* mutations are characterized by increased frequencies of *BRAF*, *KMT2D*, *HNF1A* and *BRCA2* mutations (all, q<0.001). In contrast, a lower prevalence of *APC*, *KRAS*, *CTNNB1* and *PIK3C*A mutations compared to *RNF43* WT patients was observed (all, q<0.05) **(Supplementary Figure 1)**.

Since literature is conflicting regarding the functional loss of the specific *RNF43* G659fs variant we evaluated the subset of *RNF43* G659fs patients. Of note, virtually all of these cases showed a MSI-H/dMMR (99.2%) and a high TMB (99.6%) status. A comparison of *RNF43* non-G569fs variants and *RNF43/RSPO* WT cases is displayed in **Supplementary Figure 2**.

DISCUSSION

Inappropriate activation of Wnt/β - catenin signaling is a key oncogenic event in a significant subset of CRCs (18) and is associated with tumor cell proliferation and drug resistance (19, 20). While the most frequent LOF mutation in the Wnt/β-catenin pathway, namely *APC*, has been very well studied (21), genetic alterations in the Wnt receptor complex emerged only recently as a potential new therapeutic target (21, 22). LOF mutations in *RNF43* and *RSPO* fusion proteins were described previously to occur in a small subgroup of CRCs (15, 23, 24). However, the molecular landscape of these genetic alterations in CRC remains previously unexplored. Herein, we studied the molecular profile of CRC patients harboring a *RNF43* mutation or a *RSPOfp*. Our study revealed that the molecular landscape of *RNF43*-mut CRC substantially differs from the genetic portrait of *RSPOfp* CRC. In fact, a higher rate of MSI-H/dMMR was observed in *RNF43*-mut compared to *RSPOfp*-positive tumors. This is in line with findings previously reported in the literature, that *RNF43* mutations are more frequently encountered in patients with MSI-H/dMMR cancers (15), both in sporadic cases, and, to a lesser extent, in patients with a Lynch syndrome (25). However, when focusing on the subgroup of MSS/*RNF43*-mut tumors, the genetic profile exhibited greater similarity to that observed in *RSPOfp*-positive tumors. From this first perspective this finding might indicate that a part of *RNF43* mutations might be a secondary mutation effect triggered by MSI. However, when analyzing the subset of MSI-H patients, distinct differences of the molecular landscape according to *RNF43* status were observed. Hence, it remains elusive to which extent the genomic landscape is altered either due to MSI-H/dMMR status or *RNF43* mutations.

Up to now, conflicting data exists regarding the pathogenicity of specific *RNF43* mutations. In 2019, Tu and colleagues reported that the G659fs mutation does not seem to have an impact on carcinogenesis and seems to be fully functional (26). In contrast, two studies

published in 2020 were not able to corroborate this finding (27). In particular, Yu and colleagues could show that the G659fs mutation induces LOF (16). The current uncertainty whether the G659fs mutation represents a LOF is also reflected in our analysed cohorts. In the discovery cohort the G659fs mutational variant was considered pathogenic whereas this specific mutation was excluded in the analyses of the validation cohort. Of note, we observed that virtually all patients harboring a *RNF43* G659fs mutation were characterized by a MSI-H/dMMR and a TMB-high phenotype. Up to now, the impact of the G659fs mutation on WNT activation remains elusive. Therefore, further mechanistic studies are highly desirable to unravel the pathogenic interplay between MSI-H/dMMR and different *RNF43* mutations.

To date, only limited data is available regarding prognostic significance of the respective alterations. Matsumoto and colleagues reported that *RNF43* mutations are associated with an aggressive phenotype in *BRAF*-mut CRC leading to poor outcome (28). In line with this finding, survival analysis of the discovery cohort showed that patients harboring *RNF43* mutations are characterized by inferior overall survival. Additionally, for the first time we observed that *RSPO* fusions represent a poor prognostic factor.

Anatomic location, or 'sidedness', of CRC has emerged over the past several years as an important predictive and prognostic biomarker in this cancer entity (29, 30). In particular, enrichment of mutations in *BRAF*, and also co-association with MSI-H/dMMR in right-sided CRC tumors is associated with a worse prognosis (31, 32), and many of the additional molecular factors associated with this worse outcome are under active investigation. Thus, we hypothesized that *RNF43* and/or *RSPOfp* are associated with this genomic signature. In pursing this hypothesis, we detected a higher prevalence of *RNF43* mutations in right-sided CRC primaries compared to tumors originating in left-sided locations irrespective of MSI

355 status. This observation opens further options to combinational treatment approaches in
356 this subset of patients with CRC. Indeed, in patients with MSI-H/dMMR tumors immune
357 checkpoint inhibition has been proven to be efficacious (33, 34). To date, the reasons why
358 patients with MSS cancers do not respond to immunotherapy have not been fully elucidated
359 at the cellular and molecular levels, so far. Besides the hypothesis of reduced neoantigen
360 formation in MSS tumors (35), other authors have reported that T-cells are actively excluded
361 from the tumor (36). One possible pathway that modulating T-cell activity is the Wnt
362 pathway, whose activation has been shown to prevent anti-tumor response in melanoma
363 (37). Hence, inhibition of Wnt signaling seems to activate the immune system by activating
364 dendritic cells as well as T-cells (38, 39).
365 Many studies reported, that *RSPOfp* alterations do not occur in tumors with *APC* mutations
366 (6, 15), although it is not clear if *RSPOfp* mutations have a functional redundancy with *APC*
367 mutations. However, in both (experimental and validation) cohorts, we observed that some
368 *RNF43*-mut/*RSPOfp*-positive tumors harbor co-mutations in *APC*, which represents a novel
369 finding.
370 Furthermore, despite the observation that Wnt/β-catenin activation is one of the key drivers
371 of tumorigenesis in CRC, inhibition of the Wnt/β-catenin pathway has not been proven to be
372 an efficacious therapeutic strategy to date (40). However, new attempts are being made to
373 efficiently target the Wnt/β-catenin signaling pathway. One strategy could consist of
374 inhibiting ligand-mediated activation of the Wnt/β-catenin cascade by PORCN inhibitors in
375 CRC patients carrying *RSPO* rearrangements (17). For the *RNF43* G659fs mutation as a
376 predictive marker for a Wnt/β-catenin inhibiting treatment is still inconclusive, as some
377 authors suggest that this mutation does not alter the protein's function (26, 41). However,
378 others provide evidence that this frameshift mutation leads to a responsiveness to PORCN

inhibition (16). Other strategies may include to target the DKK-1, a modulator of Wnt/β-catenin activity (42), for which the monoclonal antibody DKN-01 is currently under clinical investigation in several gastrointestinal malignancies (e.g. NCT04057365 or NCT04166721) or targeting the Wnt co-receptor LRP5/6 for which the inhibitor BI905677 is currently under early clinical investigation (NCT03604445). Moreover, drugs directly blocking the interaction of β-catenin and CREB are currently being investigated in clinical trials (43). Taken together, it is tempting to speculate that the emergence of effective Wnt/β-catenin inhibitors, such as the PORCN inhibitors LGK974 (44), ETC-159 (45), or CGX1321 (41) might reshape the immunologic sensitivity of a subset of CRCs overcoming resistance to immunotherapeutical approaches, especially in the MSS subcohorts.

Several limitations apply to our study: 1.) Validation of our findings regarding *RSPO* rearrangements was not feasible, since in the validation cohort no fusion panel analysis was performed. 2.) Due to the retrospective study design a potential selection bias might have existed. 3.) Lacking the option of prospective longitudinal analyses we were not able to account for the possibility of sub-clonal *RNF43* mutations. 4.) Due to limited availability of tissue and specific restrictions, no additional IHC stainings, depicting a variety of immunogenic markers and immune cell infiltration, and respective correlation with *RNF43/RSPO* status, could be conducted. Future prospective trials using sequential analyses during the molecular patient journey and further techniques (i.e. liquid biopsy, single-cell analysis) are desirable to dismantle the above mentioned limitations.

Taken together, in this large cohort of CRC patients whose tumors underwent molecular profiling we have identified a significant subset of CRCs harboring a *RNF43* mutation or a *RSPO* fusion protein which are characterized by a distinct genetic landscape. Thus, these detectable gene alterations represent a potential new therapeutic target and several clinical

403 trials are currently ongoing to prove the efficacy of different Wnt/β-catenin signaling
404 inhibitors in *RNF43/RSPO*-positive tumors. Furthermore, MSI-H/dMMR were observed in a
405 subgroup of *RNF43*-mutated tumors suggesting that immune checkpoint inhibition with and
406 without Wnt/β-catenin signaling inhibitors may be a reasonable combinational therapeutic
407 approach that should be tested in prospective trials.
408
409
410
411
412
413 **Authors' contributions**
414 The authors confirm contribution to the paper as follows: study conception and design: AS,
415 FB, FK, ZT, EL, HJL ; data collection: YB, JX, JS, ME, WMK, KHL, GST, HT, SHL, HLN; analysis and
416 interpretation of results: AS, FK, PES, FB, JX, KZ, ZT, DR, DW, GS, VND, YB; draft manuscript
417 preparation: AS, AP, KZ, FK, HJL, WMK, AA, MDB, DW, EL, RMG, AG, AFS, JLM, BAW. All
418 authors reviewed the results and approved the final version of the manuscript.
419

REFERENCES

1. Siegel RL, Miller KD, Jemal A. Cancer statistics, 2020. CA Cancer J Clin. 2020;70(1):7-30.
2. Malvezzi M, Carioli G, Bertuccio P, Boffetta P, Levi F, La Vecchia C, et al. European cancer mortality predictions for the year 2018 with focus on colorectal cancer. Ann Oncol. 2018;29(4):1016-22.
3. Hinoi T, Akyol A, Theisen BK, Ferguson DO, Greenson JK, Williams BO, et al. Mouse model of colonic adenoma-carcinoma progression based on somatic Apc inactivation. Cancer Res. 2007;67(20):9721-30.
4. Sansom OJ, Reed KR, Hayes AJ, Ireland H, Brinkmann H, Newton IP, et al. Loss of Apc in vivo immediately perturbs Wnt signaling, differentiation, and migration. Genes Dev. 2004;18(12):1385-90.
5. Dow LE, O'Rourke KP, Simon J, Tschaharganeh DF, van Es JH, Clevers H, et al. Apc Restoration Promotes Cellular Differentiation and Reestablishes Crypt Homeostasis in Colorectal Cancer. Cell. 2015;161(7):1539-52.
6. Seshagiri S, Stawiski EW, Durinck S, Modrusan Z, Storm EE, Conboy CB, et al. Recurrent R-spondin fusions in colon cancer. Nature. 2012;488(7413):660-4.
7. Han T, Schatoff EM, Murphy C, Zafra MP, Wilkinson JE, Elemento O, et al. R-Spondin chromosome rearrangements drive Wnt-dependent tumour initiation and maintenance in the intestine. Nat Commun. 2017;8:15945.
8. de Lau W, Peng WC, Gros P, Clevers H. The R-spondin/Lgr5/Rnf43 module: regulator of Wnt signal strength. Genes Dev. 2014;28(4):305-16.
9. Min BH, Hwang J, Kim NK, Park G, Kang SY, Ahn S, et al. Dysregulated Wnt signalling and recurrent mutations of the tumour suppressor RNF43 in early gastric carcinogenesis. J Pathol. 2016;240(3):304-14.
10. Ryland GL, Hunter SM, Doyle MA, Rowley SM, Christie M, Allan PE, et al. RNF43 is a tumour suppressor gene mutated in mucinous tumours of the ovary. J Pathol. 2013;229(3):469-76.
11. Wang K, Yuen ST, Xu J, Lee SP, Yan HH, Shi ST, et al. Whole-genome sequencing and comprehensive molecular profiling identify new driver mutations in gastric cancer. Nat Genet. 2014;46(6):573-82.
12. Jiao Y, Yonescu R, Offerhaus GJ, Klimstra DS, Maitra A, Eshleman JR, et al. Whole-exome sequencing of pancreatic neoplasms with acinar differentiation. J Pathol. 2014;232(4):428-35.
13. Waddell N, Pajic M, Patch AM, Chang DK, Kassahn KS, Bailey P, et al. Whole genomes redefine the mutational landscape of pancreatic cancer. Nature. 2015;518(7540):495-501.
14. Eto T, Miyake K, Nosho K, Ohmuraya M, Imamura Y, Arima K, et al. Impact of loss-of-function mutations at the RNF43 locus on colorectal cancer development and progression. J Pathol. 2018;245(4):445-55.
15. Giannakis M, Hodis E, Jasmine Mu X, Yamauchi M, Rosenbluh J, Cibulskis K, et al. RNF43 is frequently mutated in colorectal and endometrial cancers. Nat Genet. 2014;46(12):1264-6.
16. Yu J, Yusoff PAM, Woutersen DTJ, Goh P, Harmston N, Smits R, et al. The Functional Landscape of Patient-Derived RNF43 Mutations Predicts Sensitivity to Wnt Inhibition. Cancer Res. 2020;80(24):5619-32.
17. Koo BK, van Es JH, van den Born M, Clevers H. Porcupine inhibitor suppresses paracrine Wnt-driven growth of Rnf43;Znrf3-mutant neoplasia. Proc Natl Acad Sci U S A. 2015;112(24):7548-50.

18. Nusse R, Clevers H. Wnt/β-Catenin Signaling, Disease, and Emerging Therapeutic Modalities. Cell. 2017;169(6):985-99.
19. Moradi A, Ghasemi F, Anvari K, Hassanian SM, Simab SA, Ebrahimi S, et al. The cross-regulation between SOX15 and Wnt signaling pathway. J Cell Physiol. 2017;232(12):3221-5.
20. Yuan S, Tao F, Zhang X, Zhang Y, Sun X, Wu D. Role of Wnt/β-Catenin Signaling in the Chemoresistance Modulation of Colorectal Cancer. Biomed Res Int. 2020;2020:9390878. doi: 10.1155/2020/9390878.
21. Zhang L, Shay JW. Multiple Roles of APC and its Therapeutic Implications in Colorectal Cancer. J Natl Cancer Inst. 2017;109(8):djw332.
22. Jiang X, Cong F. Novel Regulation of Wnt Signaling at the Proximal Membrane Level. Trends Biochem Sci. 2016;41(9):773-83.
23. Yan HHN, Lai JCW, Ho SL, Leung WK, Law WL, Lee JFY, et al. RNF43 germline and somatic mutation in serrated neoplasia pathway and its association with BRAF mutation. Gut. 2017;66(9):1645-56.
24. Sekine S, Yamashita S, Tanabe T, Hashimoto T, Yoshida H, Taniguchi H, et al. Frequent PTPRK-RSPO3 fusions and RNF43 mutations in colorectal traditional serrated adenoma. J Pathol. 2016;239(2):133-8.
25. Fennell LJ, Clendenning M, McKeone DM, Jamieson SH, Balachandran S, Borowsky J, et al. RNF43 is mutated less frequently in Lynch Syndrome compared with sporadic microsatellite unstable colorectal cancers. Fam Cancer. 2018;17(1):63-9.
26. Tu J, Park S, Yu W, Zhang S, Wu L, Carmon K, et al. The most common RNF43 mutant G659Vfs*41 is fully functional in inhibiting Wnt signaling and unlikely to play a role in tumorigenesis. Sci Rep. 2019;9(1):18557.
27. Tsukiyama T, Zou J, Kim J, Ogamino S, Shino Y, Masuda T, et al. A phospho-switch controls RNF43-mediated degradation of Wnt receptors to suppress tumorigenesis. Nat Commun. 2020;11(1):4586.
28. Matsumoto A, Shimada Y, Nakano M, Oyanagi H, Tajima Y, Kameyama H, et al. RNF43 mutation is associated with aggressive tumor biology along with BRAF V600E mutation in right-sided colorectal cancer. Oncol Rep. 2020;43(6):1853-62.
29. Snyder M, Bottiglieri S, Almhanna K. Impact of Primary Tumor Location on First-line Bevacizumab or Cetuximab in Metastatic Colorectal Cancer. Rev Recent Clin Trials. 2018;13(2):139-49.
30. Boeckx N, Koukakis R, Op de Beeck K, Rolfo C, Van Camp G, Siena S, et al. Primary tumor sidedness has an impact on prognosis and treatment outcome in metastatic colorectal cancer: results from two randomized first-line panitumumab studies. Ann Oncol. 2017;28(8):1862-8.
31. Lee MS, Menter DG, Kopetz S. Right Versus Left Colon Cancer Biology: Integrating the Consensus Molecular Subtypes. J Natl Compr Canc Netw. 2017;15(3):411-9.
32. Gao XH, Yu GY, Gong HF, Liu LJ, Xu Y, Hao LQ, et al. Differences of protein expression profiles, KRAS and BRAF mutation, and prognosis in right-sided colon, left-sided colon and rectal cancer. Sci Rep. 2017;7(1):7882.
33. Le DT, Uram JN, Wang H, Bartlett BR, Kemberling H, Eyring AD, et al. PD-1 Blockade in Tumors with Mismatch-Repair Deficiency. N Engl J Med. 2015;372(26):2509-20.
34. André T, Shiu KK, Kim TW, Jensen BV, Jensen LH, Punt C, et al. Pembrolizumab in Microsatellite-Instability-High Advanced Colorectal Cancer. N Engl J Med. 2020;383(23):2207-18.

35. Rizvi NA, Hellmann MD, Snyder A, Kvistborg P, Makarov V, Havel JJ, et al. Cancer immunology. Mutational landscape determines sensitivity to PD-1 blockade in non-small cell lung cancer. Science. 2015;348(6230):124-8.
36. Feig C, Jones JO, Kraman M, Wells RJ, Deonarine A, Chan DS, et al. Targeting CXCL12 from FAP-expressing carcinoma-associated fibroblasts synergizes with anti-PD-L1 immunotherapy in pancreatic cancer. Proc Natl Acad Sci U S A. 2013;110(50):20212-7.
37. Spranger S, Bao R, Gajewski TF. Melanoma-intrinsic β-catenin signalling prevents anti-tumour immunity. Nature. 2015;523(7559):231-5.
38. Suryawanshi A, Manoharan I, Hong Y, Swafford D, Majumdar T, Taketo MM, et al. Canonical wnt signaling in dendritic cells regulates Th1/Th17 responses and suppresses autoimmune neuroinflammation. J Immunol. 2015;194(7):3295-304.
39. Gattinoni L, Zhong XS, Palmer DC, Ji Y, Hinrichs CS, Yu Z, et al. Wnt signaling arrests effector T cell differentiation and generates CD8+ memory stem cells. Nat Med. 2009;15(7):808-13.
40. Martin-Orozco E, Sanchez-Fernandez A, Ortiz-Parra I, Ayala-San Nicolas M. WNT Signaling in Tumors: The Way to Evade Drugs and Immunity. Front Immunol. 2019;10:2854.
41. Li C, Cao J, Zhang N, Tu M, Xu F, Wei S, et al. Identification of RSPO2 Fusion Mutations and Target Therapy Using a Porcupine Inhibitor. Sci Rep. 2018;8(1):14244.
42. Niehrs C. Function and biological roles of the Dickkopf family of Wnt modulators. Oncogene. 2006;25(57):7469-81.
43. Emami KH, Nguyen C, Ma H, Kim DH, Jeong KW, Eguchi M, et al. A small molecule inhibitor of beta-catenin/CREB-binding protein transcription [corrected]. Proc Natl Acad Sci U S A. 2004;101(34):12682-7.
44. Li J, Wu G, Xu Y, Ruan N, Chen Y, Zhang Q, et al. Porcupine Inhibitor LGK974 Downregulates the Wnt Signaling Pathway and Inhibits Clear Cell Renal Cell Carcinoma. Biomed Res Int. 2020;2020:2527643. doi: 10.1155/2020/2527643.
45. Ng M, Tan DS, Subbiah V, Weekes CD, Teneggi V, Diermayr V, et al. First-in-human phase 1 study of ETC-159 an oral PORCN inhbitor in patients with advanced solid tumours. J Clin Oncol. 2017;35(15_suppl):2584 .

549 **TABLES**

550 **Table 1:** Characteristics of the discovery cohort.

Characteristic		*RSPO* fusion positive	*RNF43*-mut	*RNF43* and *RSPO* wildtype
Total – no. (%)		94 (1.3)	443 (6.1)	6,708 (92.6)
Age (years)	Median Age	61	69	62
	Range	36-90	18-93	15-98
Sex – no. (%)	Female	46 (49)	263 (59)	2,922 (44)
	Male	48 (51)	180 (41)	3,786 (56)
Tumor Location – no. (%)	Left	23 (25)	66 (15)	2,156 (32)
	Rectal	29 (31)	39 (9)	1,640 (24)
	Right	24 (26)	232 (52)	1,612 (24)
	Transverse	8 (9)	46 (10)	293 (4)
	Unclear	10 (11)	60 (13.5)	1,007 (15)

551
552
553 **Table 2:** Characteristics of the validation cohort.
554

Characteristics	**No. (%)**
CRC cases	816
***RNF43* mutation status**	
Mutated	65 (7.97)
Wildtype	751 (92.03)
Comutations in *APC*, *KRAS*, *BRAF* and *NRAS*	57 (88)
No comutation in the respective genes	8 (12)
Microsatellite status	
MSI-H/dMMR (%)	7 (11)
MSS/pMMR (%)	42 (64)
Not reported (%)	16 (25)

555
556

FIGURE LEGENDS

Figure 1: Real-world overall survival stratified by *RSPO/RNF43* status.
A) Comparison of *RSPOfp* vs. *RNF43/RSPOfp*-WT patients (*RSPOfp* vs. WT: HR 0.62, 95%CI 0.48-0.81, p<0.001).
B) Comparison of *RNF43*-mut vs. *RNF43/RSPOfp*-WT patients (HR 0.86, 95%CI 0.78-0.94, p<0.001).

Figure 2: Molecular landscape of the discovery cohort.
A) Comparison of the genetic landscape of *RNF43*-mut, *RSPOfp* and *RNF43/RSPOfp*-WT tumors. Shown are mutations that are significantly different between *RSPOfp* vs. *RNF43*-mut tumors (all q<0.05; ns: p<0.05, but q<0.05 was not reached).
B) Copy number alterations in *RNF43*-mut, *RSPOfp* and *RNF43/RSPO*-WT tumors. *q<0.05, **q<0.01, ***q<0.001.
C) MSI, TMB and PDL-1 status in *RNF43*-mut, *RSPOfp* and *RNF43/RSPOfp*-WT tumors. None of the *RSPOfp* patients showed a TMB >10 mt/Mb or a MSI-H/dMMR status.*q<0.05, **q<0.01, ***q<0.001.

Figure 3: Molecular landscape of the MSS subcohort.
A) Genetic landscape comparison between *RSPOfp* vs. *RNF43*-mut tumors in the MSS subgroup. *KRAS* mutation was the only statistically different genetic alteration. ***q<0.001.
B) TMB and PDL-1 status in *RNF43*-mut, *RSPOfp* and *RNF43/RSPOfp*-WT CRCs. None of the *RSPOfp* patients showed a TMB >10 mt/Mb or a MSI-H/dMMR status.*q<0.05, **q<0.01, ***q<0.001.
C) Copy number alterations in *RNF43* mutations, *RSPO rearrangements* and *RNF43/RSPO*-WT samples. *q<0.05.

Figure 1: Real-world overall survival stratified by *RSPO/RNF43* status.

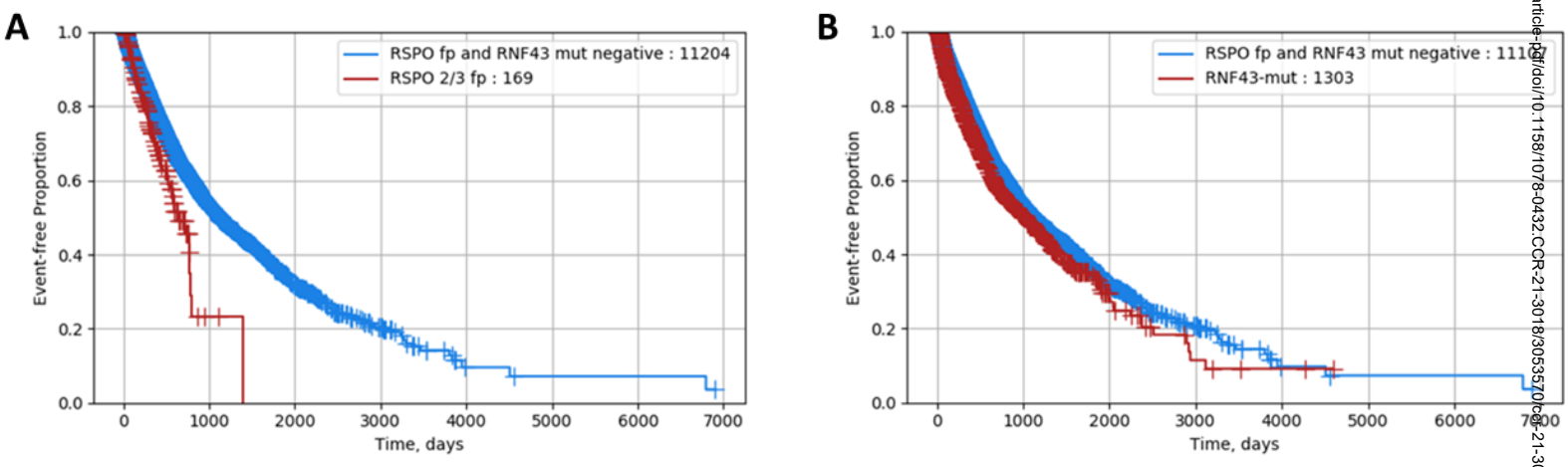

Figure 2: Molecular landscape of the discovery cohort.

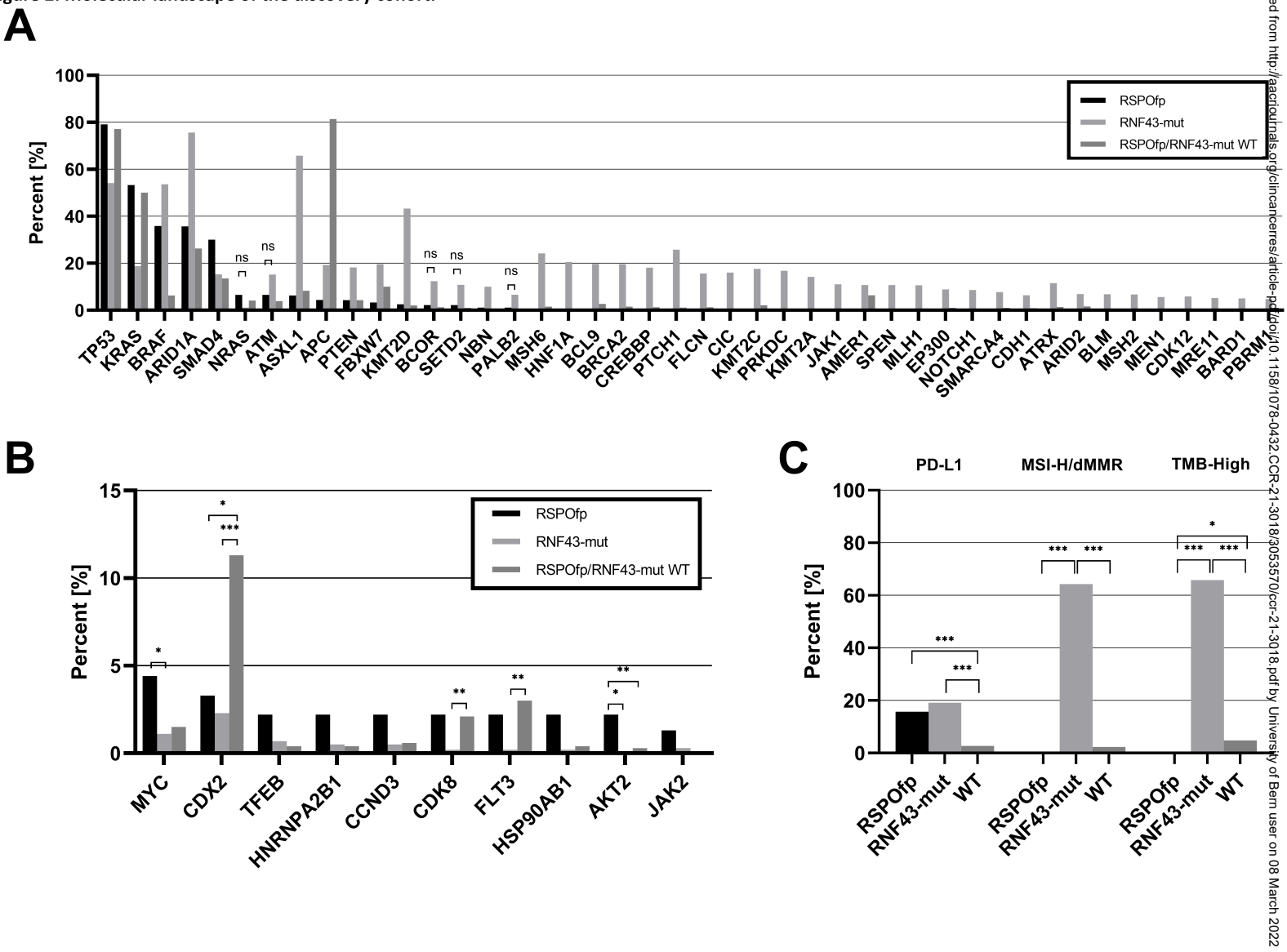

Figure 3: Molecular landscape of the MSS subcohort.